Profiling the Interface Electron Gas of $LaAlO_3/SrTiO_3$ Heterostructures with Hard X-Ray Photoelectron Spectroscopy

M. Sing,[1] G. Berner,[1] K. Goß,[1] A. Müller,[1] A. Ruff,[1] A. Wetscherek,[1] S. Thiel,[2] J. Mannhart,[2] S. A. Pauli,[3]
C. W. Schneider,[3] P. R. Willmott,[3] M. Gorgoi,[4] F. Schäfers,[4] and R. Claessen[1]

[1]*Experimentelle Physik 4, Universität Würzburg, Am Hubland, D-97074 Würzburg, Germany*
[2]*Institute of Physics, Universität Augsburg, Electronic Correlations and Magnetism, Experimentalphysik VI,
Universitätsstrasse 1, D-86135 Augsburg, Germany*
[3]*Paul Scherrer Institut, CH-5232 Villigen, Switzerland*
[4]*Berliner Elektronenspeicherring-Gesellschaft für Synchrotronstrahlung m.b.H.,
Albert-Einstein-Strasse 15, D-12489 Berlin, Germany*
(Received 5 September 2008; published 30 April 2009)

The conducting interface of $LaAlO_3/SrTiO_3$ heterostructures has been studied by hard x-ray photoelectron spectroscopy. From the Ti $2p$ signal and its angle dependence we derive that the thickness of the electron gas is much smaller than the probing depth of 4 nm and that the carrier densities vary with increasing number of $LaAlO_3$ overlayers. Our results point to an electronic reconstruction in the $LaAlO_3$ overlayer as the driving mechanism for the conducting interface and corroborate the recent interpretation of the superconducting ground state as being of the Berezinskii-Kosterlitz-Thouless type.

Novel phases with often unexpected electronic and magnetic properties may form at the interfaces of epitaxial heterostructures made out of complex insulating oxides. A case in point is $LaAlO_3$ (LAO) on TiO_2-terminated $SrTiO_3$ (STO), for which a metallic interface state was found at room temperature (RT) [1]. While two-dimensional (2D) superconducting behavior below 200 mK [2,3] and indications of ferromagnetism below $\sim$1 K [4] have been reported, the origin and nature of the metallic state have been matters of intense debate [1,2,4–13]. The metallic state could either be of extrinsic origin, i.e., due to effective n doping by oxygen vacancies, or be intrinsic, i.e., owing to electronic reconstruction. In the latter case, the polar structure of LAO with alternating $(LaO)^+$ and $(AlO_2)^-$ planes leads to a monotonically increasing potential with an increasing number of monolayers [5]. To avoid this polar catastrophe, in the most simple picture half an electron charge per 2D unit cell is transferred to the interface [14], corresponding to a sheet carrier density $n_{2D} \approx 3.4 \times 10^{14}$ cm^{-2}. However, depending on sample growing conditions, in particular, the oxygen partial pressure during deposition, experimentally determined sheet carrier densities of $\sim 10^{13}$–10^{17} cm^{-2} [4,8,10,13,15] have been measured. Likewise, considerable efforts have been made to determine the thickness of the conducting layer. Values between 7 nm and 600 μm were found [2,5,9,10,13,16]. Unfortunately, simultaneous information on layer thickness and charge carrier concentration is scarce [2,10,13].

In this Letter, we present for the first time direct spectroscopic evidence for the two-dimensional electron gas (2DEG), using hard x-ray photoelectron spectroscopy (HAXPES). From the Ti^{3+} signal in the $2p$ core-level spectra, we have a clear indication for extra electrons located at Ti sites. We are further able to extract information on layer thickness and carrier density on an equal footing. It is found that the surplus interface charge is confined to a thickness considerably smaller than the photoemission probing depth, probably to one unit cell only. The charge density per unit area increases strongly with the number of LAO overlayer unit cells. We also observe the creation of extrinsic charge carriers by x-ray exposure. Our results are in favor of electronic reconstruction in the LAO overlayer instead of band bending as the driving cause for the 2DEG formation. The very small 2DEG thickness confirms the generically 2D nature of the transition into a superconducting ground state which has recently been proposed for identically prepared samples [2].

LAO/STO heterostructures have been grown by pulsed laser deposition on TiO_2-terminated (001) STO surfaces. One set of samples—with 2, 4, 5, and 6 unit cell (uc) thick LAO overlayers—was grown at the University of Augsburg as described elsewhere [8]. Here we only point out that, after deposition in an O_2 atmosphere of 2×10^{-5} mbar around $800\,°C$, these samples were cooled to RT in 400 mbar of O_2 with an extra 1 h oxidation step at $600\,°C$ (these samples are denoted "Augsburg samples" throughout this Letter) in order to avoid oxygen vacancies. The other sample is 5 uc thick and was prepared at the Paul Scherrer Institute under 5×10^{-6} mbar of O_2 and otherwise similar conditions. This sample was not subject to a particular oxidation treatment (it is henceforth denoted the "PSI sample") and is the same as that used in Ref. [16].

Hard x-ray photoemission was performed at beam line KMC-1 [17] of the synchrotron BESSY using the end station HIKE. The total energy resolution using 3 keV
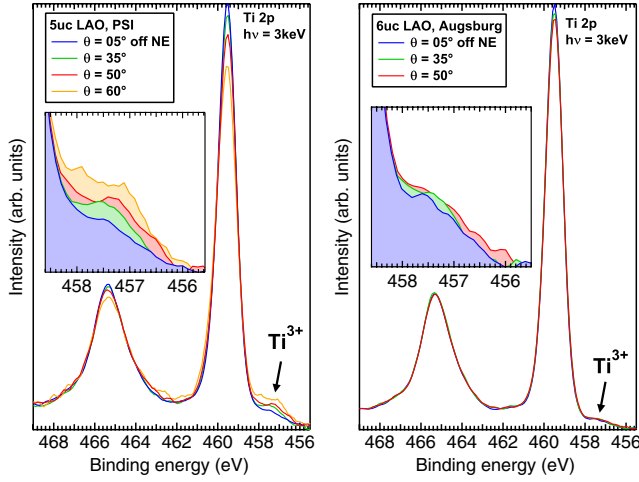
FIG. 1 (color online).   Ti $2p$ spectra of two different LAO/STO samples for various emission angles θ.
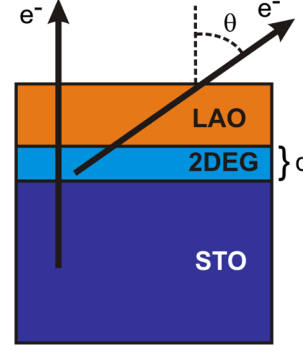

FIG. 2 (color online).   Schematic illustrating depth profiling by angle-dependent HAXPES.

the damping in the LAO overlayer does not change this ratio anymore but only results in an absolute reduction of the signal):

$$\frac{I(3+)}{I(4+)} = \frac{p[1 - \exp(-d/\lambda\cos\theta)]}{1 - p[1 - \exp(-d/\lambda\cos\theta)]}. \quad (1)$$

For $d \gg \lambda$, Eq. (1) reduces to $I(3+)/I(4+) = p/(1 - p)$, which means that there is no angular dependence in this case. Note that in Eq. (1) p and d are not independent. However, due to the exponentials d reacts very sensitively to a small variation of p except in the limit $d \ll \lambda$, implying that the parameter range for p and d can be narrowed effectively by comparison with experiment.

This is illustrated in Fig. 3, where we show the angle dependence of the $I(3+)/I(4+)$ ratio for several LAO/STO samples, as obtained by a standard fitting procedure. The shaded areas mark the array of curves according to Eq. (1) falling within the error bars ($\pm20\%$) of the experimental $I(3+)/I(4+)$ ratios. The corresponding parameter ranges for p and d are indicated in Fig. 3 and listed in Table I for all samples. Also drawn are best fit curves (solid lines). The electron escape depth λ in STO was fixed to 40 Å according to the NIST database [18] and experimental findings on other insulating oxide compounds [19–21]. As can be seen

photons amounted to ≈500 meV. Binding energies were calibrated with reference to the Au $4f$ core level at 84.0 eV. Because of the large probing depth, no particular surface preparation was necessary. The Augsburg 4 uc sample has been contacted as described in Ref. [8] and allowed for *in situ* conductivity measurements. All data were recorded at RT and were normalized to the background intensity at higher binding energies or, equivalently, to equal integrated intensity.

In Fig. 1, HAXPES spectra are presented of the Ti $2p$ doublet at different emission angles θ with respect to the surface normal (normal emission—NE). The data sets were recorded on PSI (left panel) and Augsburg (right panel) samples exhibiting an interface 2DEG. The low spectral weight at the lower binding energy side of the main line, detailed in the insets in Fig. 1, can be attributed to emission from the $2p$ level of Ti^{3+} as evidenced by its energetic shift of 2.2 eV. Thus it represents a direct manifestation of additional electrons hosted in the otherwise empty $3d$ shell of Ti^{4+} in STO. We note that this has not been seen before with soft x-ray PES due to the insufficient probing depth [12]. By going to larger emission angles—which corresponds to a decrease in the effective electron escape depth as $\lambda_{eff} = \lambda\cos\theta$ (see Fig. 2)—the Ti^{3+} signal increases in relation to the Ti^{4+} main line. From these observations we deduce that the extra electrons are localized at the STO side of the LAO/STO interface within a region considerably smaller than the electron escape depth.

For a more quantitative analysis we use the following simple model (cf. Fig. 2): The 2DEG extends from the interface to a depth d into the STO substrate. The interface region is stoichiometric and characterized by a constant fraction p of Ti^{3+} ions per unit cell. Taking into account the exponential damping factor $e^{-z/\lambda_{eff}}$ for photoelectrons created in depth z, one can easily calculate the ratio of Ti^{3+} to Ti^{4+} signal as a function of emission angle θ (note that
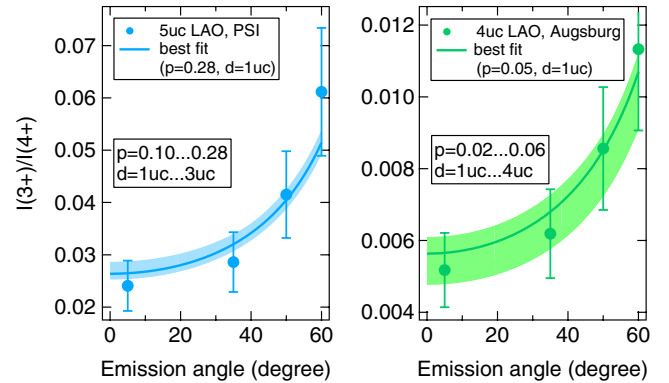

FIG. 3 (color online).   Experimental $I(3+)/I(4+)$ ratios for two LAO/STO samples as a function of angle.

TABLE I.   Parameters characterizing the LAO/STO interface electron gases from the analysis of the HAXPES data. For details, see text.

Sample	2 uc Augsburg	4 uc Augsburg	5 uc Augsburg	6 uc Augsburg	5 uc PSI
p (best fit)	0.01	0.05	0.02	0.02	0.28
p range	$0.01\ldots0.02$	$0.02\ldots0.06$	$0.02\ldots0.09$	$0.02\ldots0.11$	$0.1\ldots0.28$
d (uc) (best fit)	3	1	6	8	1
d range (uc)	$1\ldots3$	$1\ldots4$	$1\ldots8$	$1\ldots10$	$1\ldots3$
n_{2D} (10^{13} cm^{-2})	2.1	3.9	8.1	11.1	20.0

from the parameter ranges compatible with the data, the 2DEG thickness amounts to only a few STO unit cells. The carrier concentration is far below the expected $0.5e^-$ per 2D unit cell derived from simple electrostatics. From the best fit curves there is even a clear trend discernible of the 2DEG being confined to only 1 uc.

We now turn to a qualitative comparison of the different samples based on their HAXPES spectra. Figure 4 displays Ti $2p_{3/2}$ spectra (left panel) and their Ti^{3+}-related part (right panel) at an emission angle of 50°. For a bare STO substrate there is no sign of Ti^{3+}-related spectral weight, while there is small but finite weight discernible for all other samples. The Ti^{3+} intensity steadily increases with the number of LAO overlayers for the Augsburg samples and has a maximum for the PSI 5 uc sample.

It is noteworthy that the 2 uc sample exhibits finite charge carrier concentration, although from transport it is insulating [8]. The finite charge density is in line with *in situ* conductivity measurements on a 4 uc sample which shows a sharp increase by roughly a factor of 2 upon x-ray exposure. After switching the x rays off, the conductivity relaxes with a time constant of several hours. Interestingly, the bare STO substrate does not show any sizable Ti^{3+} spectral weight indicating that the LAO/STO interface is important to collect the mobile amount of photogenerated electrons. It was argued that in the polar discontinuity model the electric potential which accumulates across the LAO overlayer must first reach a critical value before the activation energy for LAO electrons to move to the interface is overcome. This argument offers an explanation for why highly mobile photogenerated electrons are confined to the interface already below the critical LAO thickness of 4 uc while they are freely distributed and not seen in HAXPES in the case of bare SrTiO$_3$ with no buried interface. We remark that part of the finite charge carrier concentration in the insulating 2 uc sample may be of an intrinsic origin but not lead to conduction. From the 2DEG thickness ranges in Table I, a tendency towards increasing thickness with increasing charge carrier concentration can be inferred. It is well conceivable that a minimal number of carriers is needed for coherent conduction. Indeed, in recent density-functional calculations of the interface electronic structure, two types of charge carriers were found [22]. The first is hosted by a 2D band, confined to one interface layer and hence particularly susceptible to local-

ization by disorder or electron phonon coupling, while the other occupies Bloch states, delocalized over several interface layers, and will contribute to transport.

To extract total charge carrier concentrations n_{2D}, one has to divide $p \cdot d$ as obtained from the best fit curves by a^2, where a is the STO lattice constant. The resulting values for n_{2D} are summarized in Table I. The difference between the 5 uc Augsburg and PSI samples by a factor of 2.5 is conspicuous. Because of the lower O$_2$ partial pressure during growth and the absence of an extra oxidation step, one might invoke extrinsic doping by oxygen vacancies as an explanation. However, in this case one would expect a much more extended electron gas owing to their high diffusion rates [23]. Rather, the subtle stoichiometric changes across the interface region previously found on this sample [16] may be responsible for the high charge carrier density.

In the Augsburg samples n_{2D} increases with the number of LAO overlayers, at variance with Hall measurements. A jump at a critical thickness of 4 uc is observed followed by a plateau reaching up to 15 uc [8]. This discrepancy could be due to the fact that the photogenerated charge carrier contribution is not constant, since with increasing LAO thickness and concomitant increasing electric potential more electrons photoexcited to trap states are released. On the other hand, a further increase of the charge carrier concentration does not necessarily have to result in a higher conductivity if the additionally occupied states are localized, as outlined above.

The thickness of the conducting layer and the charge carrier concentration are key quantities in gaining infor-
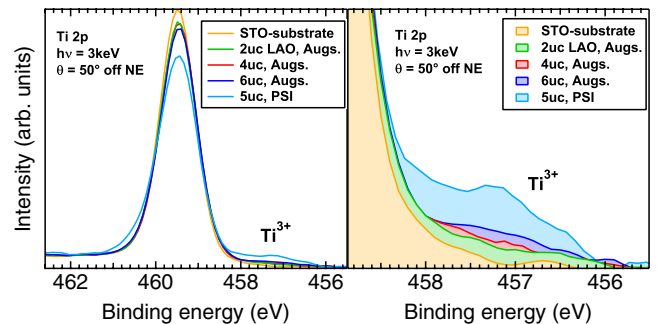

FIG. 4 (color online).   Ti $2p$ spectra of various samples plus bare STO at a fixed emission angle.

mation on both the mechanism responsible for the formation of the 2DEG as well as the nature of the possible ground states. We note that the existence of a critical LAO thickness regarding metallic conductivity precludes any scenario for the 2DEG formation in the Augsburg samples which is solely based on extrinsic mechanisms such as oxygen deficiencies, interface mixing, or interface off-stoichiometry. Recently, based on core-level shifts seen in soft x-ray PES for varying numbers of LAO overlayers, it was argued that conventional band bending induces the mobile charge carriers [12]. The fact that no signal from the metallic states at the chemical potential could be detected was used to derive a lower limit for the 2DEG thickness of 5 nm, at variance with our results. Using qualitative textbook arguments, one expects a decrease of the space charge region with decreasing dielectric constant and increasing charge carrier concentration. The dielectric constant of $SrTiO_3$ strongly decreases with increasing electric field [24]. From this and the charge carrier densities given in Table I, in a band-bending scenario, the interface thickness should decrease with the number of LAO overlayers, whereas the opposite trend is observed (Table I). Hence, we exclude band bending as the driving force for the formation of the 2DEG in our samples.

A scenario in which electronic reconstruction neutralizes the polar catastrophe matches our data better. In this picture, the interface electron gas can be confined to a region as thin as a unit cell, because the corresponding charge compensation can take place over the entire LAO overlayer, which acts as a series of parallel-plate capacitors [14]. A charge transfer that is smaller than $0.5e^-$ per 2D unit cell on the outer "plates" can be explained, e.g., by polar lattice distortions, which screen the local electric field and reduce the band discontinuity [5,25], or by surface adsorbates, which on samples exposed to air are always present. Here we emphasize that we measure the samples without any surface preparation and in the lateral center of the surface. The latter aspect distinguishes our results from determinations of the 2DEG thickness by spatially resolved methods [5,13] which probe the side faces after mechanical treatment and may be affected by fringe field effects. In such techniques, significantly larger thicknesses of the 2DEG ($\sim$7 nm) are observed.

For the ground state both a magnetic [4] and a superconducting [2] phase have been reported. While in one study it was argued that the logarithmic temperature dependence of the sheet resistance might be indicative of scattering of free charge carriers at magnetic centers (Kondo effect), the other study reported at $\approx$200 mK a resistance drop by several orders of magnitude. The transition could consistently be explained as a Berezinskii-Kosterlitz-Thouless crossover transition into a superconducting state, a scenario generic for 2D systems, in which

long-range ordering is forbidden [26]. A strict upper limit for the thickness of the conducting layer of $\cong$10 nm was inferred. Our data on essentially the same samples strongly support this conclusion. On the other hand, the Kondo scenario is not linked to low dimensionality. One thus might conjecture that either ground state is possible, depending on the 2DEG thickness as compared to the coherence lengths for superconductivity and magnetic order, respectively [3].

In summary, we depth-profiled the interface electron gas of LAO/STO heterostructures by means of angle-dependent HAXPES. We find that the 2DEG indeed is confined to one or at most a few STO unit cells. The extracted carrier sheet densities are in fair agreement with previous Hall measurements. Our data support electronic reconstruction as the driving force for the 2DEG formation and are consistent with recent reasonings on the nature of the superconducting ground state.

[1] A. Ohtomo and H. Y. Hwang, Nature (London) **427**, 423 (2004).
[2] N. Reyren et al., Science **317**, 1196 (2007).
[3] A. D. Caviglia et al., Nature (London) **456**, 624 (2008).
[4] A. Brinkman et al., Nature Mater. **6**, 493 (2007).
[5] N. Nakagawa et al., Nature Mater. **5**, 204 (2006).
[6] M. Huijben et al., Nature Mater. **5**, 556 (2006).
[7] R. Pentcheva and W. E. Pickett, Phys. Rev. B **74**, 035112 (2006).
[8] S. Thiel et al., Science **313**, 1942 (2006).
[9] G. Herranz et al., Phys. Rev. Lett. **98**, 216803 (2007).
[10] W. Siemons et al., Phys. Rev. Lett. **98**, 196802 (2007).
[11] V. Vonk et al., Phys. Rev. B **75**, 235417 (2007).
[12] K. Yoshimatsu et al., Phys. Rev. Lett. **101**, 026802 (2008).
[13] M. Basletic et al., Nature Mater. **7**, 621 (2008).
[14] C. Noguera, J. Phys. Condens. Matter **12**, R367 (2000).
[15] A. Kalabukhov et al., Phys. Rev. B **75**, 121404(R) (2007).
[16] P. R. Willmott et al., Phys. Rev. Lett. **99**, 155502 (2007).
[17] F. Schäfers et al., Rev. Sci. Instrum. **78**, 123102 (2007).
[18] NIST Standard Reference Database 71, version 1.1.
[19] C. Dallera et al., Appl. Phys. Lett. **85**, 4532 (2004).
[20] M. Sacchi et al., Phys. Rev. B **71**, 155117 (2005).
[21] H. Wadati et al., Phys. Rev. B **77**, 045122 (2008).
[22] Z. S. Popović et al., Phys. Rev. Lett. **101**, 256801 (2008).
[23] T. Ishigaki et al., J. Solid State Chem. **73**, 179 (1988).
[24] R. A. van der Berg et al., Appl. Phys. Lett. **66**, 697 (1995).
[25] R. Pentcheva and W. E. Pickett, Phys. Rev. B **78**, 205106 (2008).
[26] N. D. Mermin and H. Wagner, Phys. Rev. Lett. **17**, 1133 (1966).